



## Local cortical surface complexity maps from spherical harmonic reconstructions<sup>☆</sup>

Rachel A. Yotter<sup>a,\*</sup>, Igor Nenadic<sup>a</sup>, Gabriel Ziegler<sup>a</sup>, Paul M. Thompson<sup>b</sup>, Christian Gaser<sup>a</sup>

<sup>a</sup> Department of Psychiatry, Friedrich-Schiller University, D-07743 Jena, Germany

<sup>b</sup> Laboratory of Neuro Imaging, Department of Neurology, UCLA School of Medicine, Los Angeles, CA 90095, USA

### ARTICLE INFO

#### Article history:

Received 8 October 2010

Revised 1 February 2011

Accepted 1 February 2011

Available online 17 February 2011

#### Keywords:

Complexity  
Shape analysis  
Gyrification  
Morphology  
Schizophrenia  
MRI

### ABSTRACT

Altered cortical surface complexity and gyrification differences may be a potentially sensitive marker for several neurodevelopmental disorders. We propose to use spherical harmonic (SPH) constructions to measure cortical surface folding complexity. First, we demonstrate that the complexity measure is accurate, by applying our SPH approach and the more traditional box-counting method to von Koch fractal surfaces with known fractal dimension (FD) values. The SPH approach is then applied to study complexity differences between 87 patients with DSM-IV schizophrenia (with stable psychopathology and treated with antipsychotic medication; 48 male/39 female; mean age = 35.5 years, SD = 11.0) and 108 matched healthy controls (68 male/40 female; mean age = 32.1 years, SD = 10.0). The global FD for the right hemisphere in the schizophrenia group was significantly reduced. Regionally, reduced complexity was also found in temporal, frontal, and cingulate regions in the right hemisphere, and temporal and prefrontal regions in the left hemisphere. These results are discussed in terms of previously published findings. Finally, the anatomical implications of a reduced FD are highlighted through comparison of two subjects with vastly different complexity maps.

© 2011 Elsevier Inc. All rights reserved.

### Introduction

In clinical neuroscience, the brains of individuals with a neurological or psychiatric disorder are often found to be structurally different from the brains of healthy subjects. Furthermore, patterns of systematic structural differences have been found to be consistent for subjects with a given disorder, such that the pattern of differences depends on the specific disease. Detection of characteristic neuroanatomical patterns in patients with psychiatric disorders is likely to lead to a variety of advances in diagnosis, treatment, and prevention of psychological illness. For instance, it is at least logically possible that early diagnosis may be made in a prodromal phase, before the onset of symptoms, allowing preventative measures to be taken so that no symptoms ever appear. Since the introduction of magnetic resonance imaging (MRI) and other imaging techniques that allow in vivo measurement of brain structure, finding specific structural differences that characterize different psychiatric and neurogenetic disorders is a real possibility.

Already, several methods have been proposed to find potentially very subtle structural differences (Thompson et al., 2004). Approaches to measure differences may either be based on 3D volumetric assessments or 3D statistical mapping of gray or white matter

structures, or may involve making measurements on 3D surface models of a structure, such as the cortex or hippocampus (MacDonald et al., 2000; Mangin et al., 1995; Morra et al., 2009; Wang et al., 2010; Xu et al., 1999). Volume-based approaches are most appropriate for measuring differences in gray matter density or in regional volumes, such as for subcortical structures. Surface-based methods can measure cortical thickness or cortical folding patterns, as well as shape or curvature measures derived from the imposed surface coordinate system (Gutman et al., 2009; Luders et al., 2006; Lui et al., 2010). Our focus here is on analyzing cortical folding patterns.

Previously, the most common approach to measuring cortical folding complexity was to use a metric such as the gyrification index (GI), which is defined as the ratio of the inner surface size to the outer surface size of an outer (usually convex) hull. The GI can be measured in two dimensions by examining cortical slices (Zilles et al., 1988), or in 3D by using a reconstructed surface mesh. However, the GI metric depends on how the outer hull is defined and how brains are normalized to reduce the effect of brain size, which may result in large differences in reported values across studies. There may also be an influence of slicing direction for measures derived from 2D sections of a 3D object – if more convolutions are apparent in a given plane of section, the measured complexity may tend to be higher. In other words, the method is not intrinsic. Another potential confound is noise in the surface reconstruction, which could artificially inflate surface area without corresponding to the underlying anatomy.

These drawbacks can be circumvented by using the fractal dimension (FD), which does not rely on defining an explicit outer

<sup>☆</sup> Funding sources: BMBF 01EV0709, BMBF 01GW0740.

\* Corresponding author at: Friedrich-Schiller University, Department of Psychiatry, 3 Jahnstrasse, 07743 Jena, Germany. Fax: +49 3641 934755.

E-mail address: [rachel.yotter@uni-jena.de](mailto:rachel.yotter@uni-jena.de) (R.A. Yotter).

hull (for a review, see Lopes and Betrouni, 2009). It has been proposed that the brain is approximately a fractal (Kiselev et al., 2003), at least over a limited range of scales (Jiang et al., 2008; Lee et al., 2004; Mandelbrot and Blumen, 1989). This property has been evaluated using voxel-based information about the shape of the white matter volume (Bullmore et al., 1994; Liu et al., 2003; Zhang et al., 2007; Zhang et al., 2006). The FD can also be applied to measure cortical folding complexity, and previous studies have shown significant differences in regional FD for psychiatric disorders such as schizophrenia (Casanova et al., 1989; Narr et al., 2004; Narr et al., 2001), obsessive-compulsive disorder (Ha et al., 2005), epilepsy (Free et al., 1996), Alzheimer's disease (King et al., 2009, 2010), multiple sclerosis (Esteban et al., 2007s, 2009), cerebellar degeneration (Wu et al., 2010), stroke (Zhang et al., 2008a), autism (Awate et al., 2008), and Williams syndrome (Thompson et al., 2005), as well as for normal development (Awate et al., 2010; Blanton et al., 2001; Kalmanti and Maris, 2007; Shyu et al., 2010; Wu et al., 2009), early-life blindness (Zhang et al., 2008b), and IQ (Im et al., 2006). Furthermore, some studies report local FD or folding differences for genetic factors such as 22q11 deletion syndrome (Schaer et al., 2008), gender (Awate et al., 2009; Luders et al., 2004), and brain size (Toro et al., 2008).

Most calculations of the cortical surface FD rely on the box-counting method, which calculates regional areas for progressively lower sampling resolutions. Since the number of vertices steadily decreases, the position of these vertices can have a large impact on the FD metric and can potentially overlook relevant cortical folding information (Free et al., 1996; King et al., 2009). This concern can be addressed by aligning sulci across subjects to approximate the same cortical location for each vertex for all subjects (Thompson et al., 1996). However, alignment is a complicated endeavor that often requires manual delineation of areas that correspond geometrically across subjects, such as gyral landmarks or cortical sulci. Another possibility is to use a series of dilated disks of different sizes to cover the surface, reducing but not eliminating orientation dependencies (Free et al., 1996).

Rather than using box-counting approaches, we propose to extract surface complexity information using spherical harmonic (SPH) reconstructions (Yotter et al., 2010). By using SPH reconstructions, the number of vertices remains the same for all reconstructed surfaces, thus reducing the influence of individual vertex alignment and avoiding the need to progressively re-grid the surface, which incurs error from interpolation. Furthermore, analysis of structural characteristics in some clinical disorders may be improved by investigating the pattern of regional differences rather than a single global metric. For instance, it has been shown that pattern classification techniques can enhance the specificity of morphometric findings (Davatzikos et al., 2005; Kawasaki et al., 2007; Soriano-Mas et al., 2007; Sun et al., 2009; Yushkevich et al., 2005).

One advantage of this approach is the use of information from multiple brain regions when developing a characteristic neuroanatomical signature. This may be helpful in studies of mental illnesses, e.g., schizophrenia, which we examine here. Using SPH-derived reconstructions, we will demonstrate that it is possible to calculate a local FD for each vertex within the reconstruction, which is the first step towards obtaining accurate neuroanatomical signatures of disease states.

This paper is divided into two parts. In the first section, we compare our SPH-derived FD values to those obtained using the more traditional box-counting approach. We then compare both measures to the ground truth. We accomplish this by analyzing “von Koch” surfaces with known FD values. Furthermore, we analyze how robust the two measures are, using a brain surface rotated around each of the three axes. In the second section, we then apply our approach to data from schizophrenia and control subjects, as an illustrative application, and to assess evidence for regional and local differences in cortical complexity. The findings from this analysis are compared to

previously published results from other methods. Finally, we discuss the implications of the cortical complexity value in clinical and structural terms.

## Methods

### Spherical harmonic approach to measuring complexity

Generally, FD is computed by finding the slope of a plot regressing  $\log(\text{area})$  versus  $\log(\text{dimension})$ , over a certain range of scales. In this regression – also called a multi-fractal plot – the dimension indicates the scale of measurement, which is varied either by sub-sampling the object, or by reducing the degree of the shape representation. When using spherical harmonic reconstructions, the plot is modified to use the maximum  $l$ -value (or degree, see Appendix) of the reconstruction, and the slope may be found by regressing  $\log(\text{area})$  versus  $\log(\text{max } l\text{-value})$  (Fig. 1). Complexity can be calculated at different scales: global, regional, and local. The global complexity is a single value for the entire hemisphere; regional or local values are a set of values for regions of interest or vertices, respectively.

To obtain these values, for each hemisphere we extracted the spherical harmonic coefficients of the central surface up to a maximum  $l$ -value of 1024.<sup>1</sup> The spherically remapped points were transformed into harmonic space using a modification of the fast Fourier transform (Kostelec et al., 2000). The Appendix gives details on the spherical harmonic analysis. Finally, the surfaces were re-parameterized using a low-distortion spherical mapping of the central surface.

Fractal dimension is calculated by finding the slope of the linear portion of the log-log plot of area versus maximum  $l$ -value. This linear portion generally occurs when the total reconstructed surface area is between 40% and 80% of the full surface area. To reduce computation time, for brain surfaces 10 separate reconstructions were chosen using maximum  $l$ -values between 11 and 29. These  $l$ -values achieved optimal results for brain surfaces, resulting in surface areas that varied from approximately 40% to 75% of the maximum surface area (Yotter et al., 2010). For the von Koch surfaces, the linear portion of the slope occurred for maximum  $l$ -values between 5 and 8; for the results shown, all four reconstructions were used to calculate the FD values.

Calculation of the global complexity value was obtained directly from the total surface area of the reconstructions. For each subject, a set of initial local values was also produced. First, complexity values for each polygon were estimated by regressing the log-log plot of normalized area of the polygon versus the maximum  $l$ -value. Second, point-wise complexity values were obtained by averaging the complexity values of all neighboring polygons. This resulted in a set of unsmoothed raw local complexity values for each subject.

For both local and global measures, the area values for the spherical harmonic reconstructions were normalized by the area values in the full-coefficient reconstruction ( $l$ -value = 1024), whose surface area deviated by an infinitesimal amount from the original surface area. Although the original surface area could be used, the full-reconstruction surface area was used for consistency across all complexity measures (local and global). For the local complexity calculation, the surface area of each polygon was normalized using the area of the matching polygon in this reconstruction. This normalization step makes the complexity value somewhat independent of the surface area of the original surface; however, since smaller brains tend to have higher levels of folding detail, it is not possible to completely remove correlations between brain size and complexity. Furthermore, the regression slope is independent of the original surface area,

<sup>1</sup> The maximum  $l$ -value does not significantly affect the complexity calculation if the full reconstruction retains most of the details of the original surface mesh (i.e., greater than approximately 128). The only effect is a shift in the  $x$ -intercept due to a different surface area for the fully reconstructed mesh.

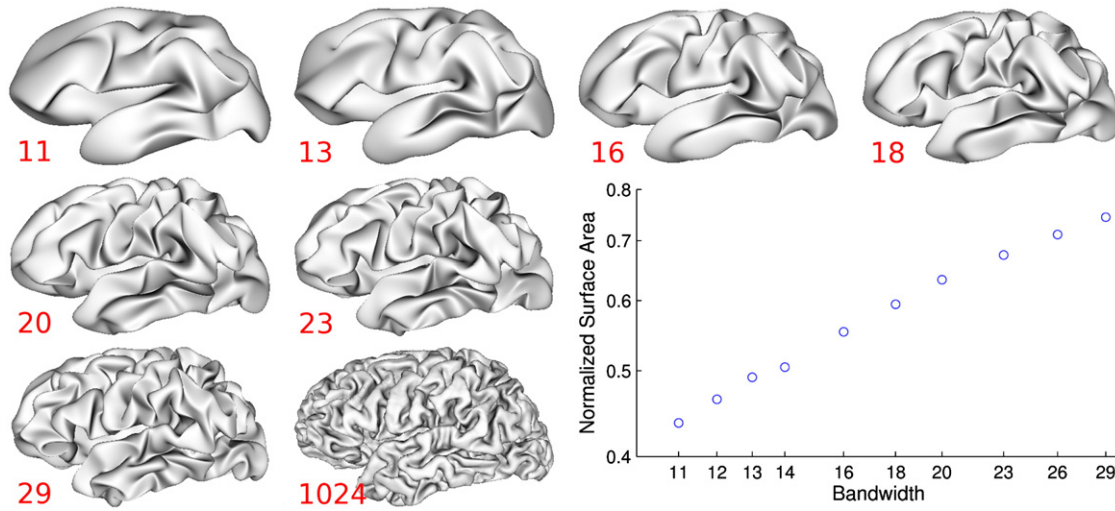


**Fig. 1.** Fractal dimension is found by finding the slope of a logarithmic plot of surface area versus the maximum  $l$ -value of the reconstruction (a measure of the bandwidth of frequencies used to reconstruct the surface shape; shown here in red font for a range of bandwidths). Surface areas are normalized by the original surface area. A linear approximation is reasonable over this range of scales.

which is reflected simply as a shift in the  $x$ -intercept of the linear approximation.

Before comparing values across subjects, local values must first be represented in a common coordinate system, which is achieved via re-parameterization of the unsmoothed raw values. This was accomplished using the registered spherical mapping for each subject (*xh.sphere.reg*), then re-parameterizing the local FD values using the *fsaverage* spherical mesh included in FreeSurfer. These values were then smoothed using a 30-mm Gaussian heat kernel (Chung et al., 2005), where the width of the smoothing filter was chosen according to the matched filter theorem. That is, the spatial frequency of the sulcal/gyral pattern suggests a filter that optimally enhances features in the range of the distance between sulci and gyri, which is about 20–30 mm.

These smoothed, registered local complexity values were then used for all statistical analyses. Regional values were obtained by averaging the complexity values associated with a particular region of interest. A flowchart of the steps taken to obtain complexity values is shown in Fig. 2.

*Box-counting approach to measuring complexity*

The definition of fractal dimension is related to the number of self-similar shapes versus the characteristic dimension, as follows:

$$FD = \frac{\log N(l)}{\log 1/l}, \tag{1}$$

where  $l$  is the characteristic dimension and  $N(l)$  is the number of self-similar shapes with dimension  $l$  required to cover the original object. Under certain conditions, namely when all objects are of uniform size

and shape, this fractal dimension value may be calculated directly; however, in most applications, there are no uniform shapes to be counted. Fortunately, the number of self-similar objects  $N(l)$  can be related to the total volume or area of the object. Since our application focuses on surface shape analysis, we are interested in area. Generally, the relationship between the number of objects  $N(l)$  and surface area  $A$  can be related as follows:

$$N(l) \propto \frac{A}{l^2}. \tag{2}$$

Thus a complexity value can be calculated using the surface area rather than the number of self-similar objects, but the values will deviate from the true Hausdorff dimension of the fractal surface if the fractal dimension were computed directly, by a factor of  $1/\log(l^2)$ .

For the box-counting method, the surface was re-sampled at progressively lower resolution, and the surface areas were normalized, so that a value of 1 indicates that the surface area of the re-parameterized surface is equivalent to the original surface area. We opted to use regular Platonic solids to avoid non-uniform re-sampling as much as possible. The FD was found by finding the slope of the linear portion of a log–log plot in which the  $x$ -axis is the dimension (or characteristic length) and the  $y$ -axis is the surface area. For all surfaces (von Koch and cortical), the re-sampling resolutions within the linear portion of the regression ranged from 80 to 5120 points. To derive the dimension, the  $x$ -axis was set to the square root of the inverse of the triangle count, which is proportional to the length of a triangle edge.

To obtain local FD values, the down-sampled reconstruction was then re-sampled back into the original coordinate space. The FD value was then calculated for each polygon by regressing  $\log(\text{area})$  versus  $\log(\text{dimension})$ , then point-wise values were calculated by averaging

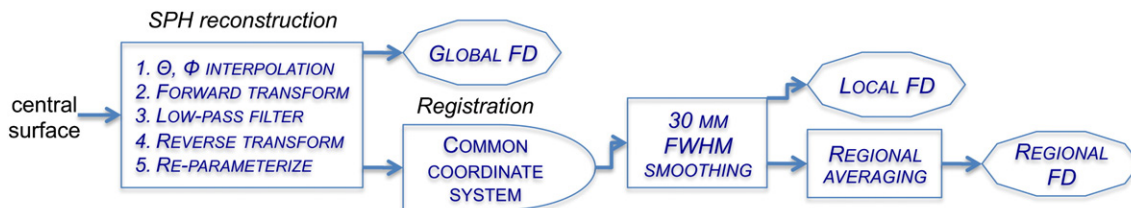


**Fig. 2.** A flowchart of the calculation process illustrates at which stages each set of complexity values are calculated. First, spherical harmonic reconstructions are derived from a central surface mesh. Area values from these reconstructions are used to directly calculate the global FD values. The area information is also re-parameterized into a common coordinate system across subjects; this data is then smoothed to derive the local FD values. Finally, regional values are averaged to obtain regional FD values.

the values of neighboring polygons. Regional FD values were obtained by averaging the local FD values for all points within the region.

All attempts were made to obtain high-quality results for the box-counting approach, including careful examination of the log–log plots, the choice of dimensions, and the inclusion of a constant offset for all values.

### von Koch surfaces

To determine whether the FD values obtained from SPH-derived reconstructions were accurate, we generated a variety of von Koch-like fractal surfaces of either tetrahedral or cubic structure. These surfaces have an FD that is computable mathematically, as well as by the SPH and box-counting algorithms. Because true von Koch surfaces result in self-intersections, the surfaces needed to be modified to avoid self-intersections, so that the Euler characteristic remained equal to 2 and the surfaces could be projected to a sphere. This was accomplished by simply reducing the length of the surface normal used to calculate the projecting structure. Specifically, the surface normal is  $l \cdot \sqrt{2/3}$  for tetrahedral and  $l$  for cubic von Koch surfaces, while the modified surfaces had normal lengths of  $l \cdot \sqrt{2/3}/s$  and  $l/s$ , respectively, where  $l$  is the characteristic dimension and  $s$  is what we will term the projection scale.

Despite this modification, the von Koch surfaces still had characteristic FD values determined by measuring the slope of a log–log plot of total surface area versus characteristic dimension (Fig. 3). The accuracy of these measurements was validated by generating a true von Koch surface and confirming that its FD value matched the theoretical value (results not shown). These FD values are the “true” values by which other approximation methods can be evaluated.

To test the ability to accurately discern local FD differences, a set of surfaces was constructed such that each of the faces used a different projection scale and thus had a unique fractal dimension.

In summary, the tetrahedral structures used six different projection scales (1.5, 2.0, 2.5, 3.0, 3.5, and 4.0) and three different characteristic dimensions or complexity levels, such that there were 18 surfaces plus three combination surfaces, which used four of the six projection scales; the cubic structures used six different projection scales and three complexity levels, resulting in 18 surfaces plus the three combination surfaces. The point resolution of all surfaces was chosen so that the number of mesh points was approximately equivalent to the number of points typically used for surface representations of cortical surface structure. For both approaches, the set of re-sampling resolutions or bandwidths was chosen so that the resultant global fractal dimension values were as closely matched

to the true fractal dimension values. Fitting of these values also included a constant offset for each value in the set.

### Statistical analysis

Statistical differences in global, regional, and local FD values were assessed using a two-tailed  $t$ -test. Regression of age and sex in the schizophrenia study did not affect the results. The resulting  $t$  values were thresholded at a  $p$ -value of  $p < 0.05$ , and local and regional values were either corrected for multiple comparisons using the False Discovery Rate (FDR) method (Benjamini and Hochberg, 1995) or left uncorrected.

### Subjects

We studied 87 patients with a DSM-IV diagnosis of schizophrenia and 108 healthy controls. The patients ( $n = 87$ ; 48 male/39 female; mean age = 35.5 years, SD = 11.0) were recruited from the Department of Psychiatry in Jena and first screened with a semi-structured interview before being assessed by two psychiatrists establishing the DSM-IV diagnosis. None of the patients had a second psychiatric, neurological or major medical condition. All patients were inpatients. None of them was in an acute episode of illness; all were in remitted clinical state, showed stable psychopathology, and were on stable antipsychotic medication. Current psychopathology in patients was assessed with the Scales for Assessment of Positive Symptoms (SAPS), and Scales for Assessment of Negative Symptoms (SANS), which was administered by an experienced and trained clinical psychiatrist (Andreasen et al., 1995). Healthy controls ( $n = 108$ ; 68 male/40 female; mean age = 32.1 years, SD = 10.0) were recruited from the city of Jena and surrounding counties and matched to the patients with regard to sex, age, and overall school/academic achievement. They were screened to exclude a concurrent or past history of psychiatric, neurological, or major medical conditions using a semi-structured interview. Further exclusion criteria for both samples included a history of head trauma, concurrent or previous substance dependence or alcoholism, and learning disability (mental retardation). All subjects were right-handed, as scored from the short version of the Edinburgh Handedness Scale (Oldfield, 1971). All participants gave written informed consent to a study protocol approved by the Ethics Committee of the Friedrich-Schiller University of Jena. Details of this patient group may be found in Nenadic et al. (2010); a subset of this sample ( $n = 12$ ) were excluded due to poor surface reconstruction quality, which was based on visual inspection and rating by an expert (G. Z.).

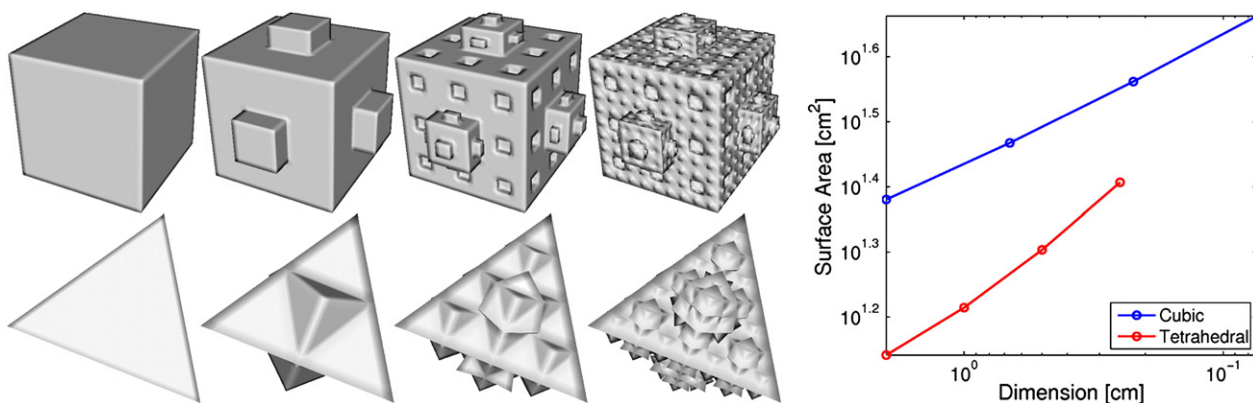


**Fig. 3.** Modified von Koch fractal surfaces with either a cubic (top row, left) or tetrahedral (bottom row, left) topology. Each set includes surfaces with progressively higher levels of detail, obtained by inserting self-similar shapes at lower dimensions. A log–log plot of surface area versus characteristic dimension (or width of the smallest feature) for three fractal levels results in a linear fit (right); the slope of this line is the characteristic FD.

## Imaging protocol

We obtained a high-resolution structural MRI for each subject on a 1.5-T Phillips Gyroscan ASCII system using a T1-weighted sequence, including 256 sagittal slices covering the entire brain (TR = 13 ms, TE = 5 ms, 25° flip angle, field of view [FOV] = 256 mm, voxel dimensions =  $1 \times 1 \times 1$  mm<sup>3</sup>) for all subjects. Foam pads were used, where appropriate, to further restrict head movement. Prior to image processing, each image was checked visually for artifacts. In addition, we used an automated tool to detect outliers implemented in the VBM8 package. All scans passed both manual and automated quality checks.

## Cortical surface extraction

Image volumes passed through a number of preprocessing steps using mostly automated procedures included in the FreeSurfer software suite, version 4.5 (<http://surfer.nmr.mgh.harvard.edu>). Details of the processing steps have been described previously (Dale et al., 1999; Fischl et al., 1999a, 1999b). In brief, images were preprocessed using intensity normalization and skull stripping, followed by normalizing the head position along the commissural axis and labeling cortical and subcortical regions. Images were then segmented, as follows (Fischl and Dale, 2000). First, images were rigid-body registered to a probabilistic brain atlas, followed by non-linear morphing to the atlas. Depending on the probability that a given location is of a particular tissue class, the intensity of the image at the location, and the local spatial configuration of the location in relation to the labels, each voxel is then assigned to one specific tissue class (gray matter, white matter, CSF, or background).

A white matter surface was derived from the white matter tissue segmentation map using the marching cubes algorithm, followed by topology correction. By outwardly deforming the white matter surface, the pial surface was also generated (Dale et al., 1999; Fischl and Dale, 2000). As a final step, the pial and white matter surfaces were averaged together, vertex-by-vertex, to construct a central surface. The central surface meshes were then used as the input for complexity analysis using our spherical harmonic approach. Before comparing local and regional values across subjects, the local FD values were re-sampled such that all values were registered to the FreeSurfer average template using the default registration algorithm (Fischl et al., 1999b).

## Validation

### Results

*Fractal dimension measurement accuracy for methods using box-counting and spherical harmonics.* The fractal dimension for the von Koch surfaces was modified by adjusting the scale used for the projecting structures, such that a projection scale value of 1.0 is a true von Koch surface and values larger than that is the ratio by which the projection scale has been reduced. This eliminates self-intersections in the structures and offers an approach to modify the fractal dimension values without large topological changes. Note that if the number of triangles or squares is plotted against the characteristic dimension, this process yields a Hausdorff dimension of 2.5849 for the tetrahedral surfaces and 2.3347 for the cubic surfaces, independent of the projection scale.

When comparing reconstructions of level-3 surfaces from the box-counting method (Fig. 4) to the SPH approach (Fig. 5), there are striking similarities. Both lose fine detail as the re-sampling resolution or the maximum *l*-value decreases. Because the SPH approach does not down-sample the mesh resolution, the reconstructions are more regular and of higher quality than those created from the box-

counting method. However, the plots of surface area versus characteristic dimension or maximum *l*-value are similar.

For all of the modified von Koch surfaces, the FD measures obtained from the SPH approach were more accurate than those derived from the box-counting method, at both the global (or overall) and regional levels (Fig. 6). For tetrahedral topologies, the resultant FD values are virtually identical to the “true” FD values, and the measurement variability over different levels of complexity is low.

Local variations in fractal dimension were simulated using von Koch fractal surfaces that had a different projection scale for each surface face. At the regional level, the SPH approach effectively measures the differences between the complexity values of each face, while the box-counting approach produces large errors, to the extent that some faces having lower complexity appear to have higher complexity. Because the spherical harmonic approach re-samples the spherical mesh at very high resolution (rather than down-sampling as with box-counting), the local fractal dimension maps are much more regular than those obtained from the box-counting approach (Fig. 7).

*Measures on a rotated cortical surface.* Validation of the measures on cortical surfaces is difficult since the approach is new and there are no cortical surfaces with precisely known fractal dimension values. However, it is possible to manipulate a cortical surface in a prescribed way, measure the change in the resulting values, and assess whether the effects coincide with expectation. One of the simplest manipulations is a rotation of the surface around rotational axes, e.g., pitch, yaw, and roll.

In theory, the complexity measure for a brain surface should remain constant, even if the surface is rotated. However, the global fractal dimension value for the box-counting approach varies widely with respect to the angle by which the surface is rotated (Fig. 8). This is clearly undesirable, as the summary measure of the properties of an object should not heavily depend upon its orientation. Furthermore, the correlation between the local FD values of rotated and un-rotated surfaces for the box-counting method only approaches a value of 1 for a rotation of 180° (Fig. 9). In contrast, the spherical harmonic derived values for global FD remain more constant, and the local FD correlation between all rotated surfaces and the un-rotated surface was never lower than 1.0.

## Discussion

*Validation of SPH approach using von Koch surfaces.* Analysis of the von Koch surfaces, whose fractal dimensions are known, demonstrated that the complexity values obtained from spherical harmonic reconstructions are generally more accurate than those obtained from the box-counting approach. Because they are less severely affected by re-sampling, interpolation, and object alignment, the resultant local complexity maps from SPH reconstructions tend to be more regular than those obtained from box-counting. This presumably makes measures more accurate and less prone to error at both the regional and global levels.

Further evidence of the improved performance of the SPH approach was obtained by simply rotating a cortical brain surface around the three cardinal axes. The large measurement differences imply that box-counting will only give measures that are comparable across subjects if brain surfaces are first carefully registered to each other, such that all re-sampled points in the down-sampled meshes roughly correspond to each other for all brain surfaces. Due to the dependence of the results on orientation of the brain, it can be presumed that box-counting would also be highly dependent upon the accuracy of the registration method employed. Conversely, the spherical harmonic approach is less dependent upon the orientation of the brain surfaces, and thus does not require careful registration in order to extract valid complexity values.

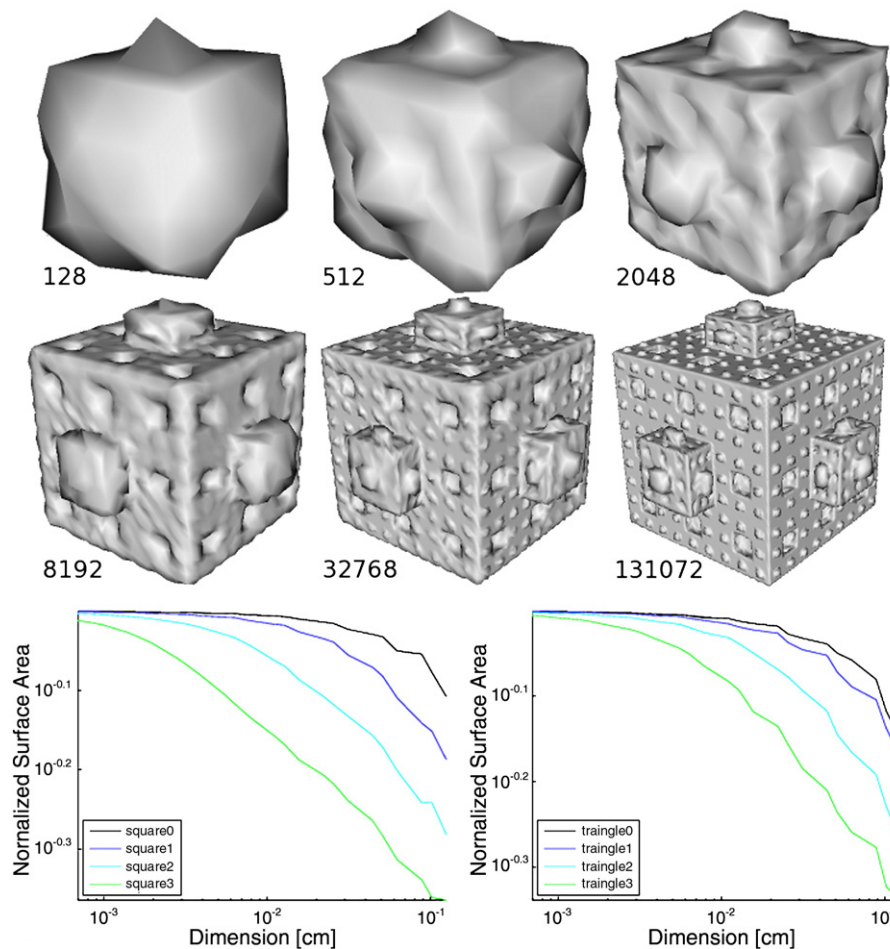


**Fig. 4.** Box-counting can measure the fractal dimension. Here we show a level-3 cubic von Koch surface with a projection scale of 2.0 re-sampled at various resolutions; the numbers indicate the triangle count in the re-sampled mesh. Below, we plot the normalized surface area versus dimension on a log–log scale, for detail levels 0–3. Fractal dimension can be estimated by measuring the slope over a range of scales that results in an approximately linear function. The area of the re-sampled surface is divided by the surface area of the original mesh.

#### Application to schizophrenia

##### Results

We detected no significant group differences between patients and controls for the global FD values in the left hemisphere (control:  $2.5820 \pm 0.0002$ ; schizophrenia:  $2.5789 \pm 0.0003$ ;  $p = 0.4252$ ), but there was a significant difference in the right hemisphere (control:  $2.5871 \pm 0.0003$ ; schizophrenia:  $2.5729 \pm 0.0003$ ;  $p = 0.0007$ ). Interestingly, there were also significant differences between groups for surface area in both hemispheres (*left hemisphere*: control:  $923.70 \text{ cm}^2$ ; schizophrenia:  $895.40 \text{ cm}^2$ ;  $p = 0.0234$ ; *right hemisphere*: control:  $925.58 \text{ cm}^2$ ; schizophrenia:  $894.91 \text{ cm}^2$ ;  $p = 0.0147$ ), but not between right and left hemispheres within groups (control:  $p = 0.8776$ ; schizophrenia:  $p = 0.9689$ ).

Regionally, the FD values in the schizophrenia group were significantly lower than those for controls, bilaterally in the precentral gyrus; in the caudal anterior cingulate gyrus and frontal pole in the left hemisphere; and the corpus callosum, lingual gyrus, and superior parietal lobe in the right hemisphere (Table 1). Patients had significantly higher regional surface complexity in the cuneus, isthmus cingulate gyrus, lateral orbitofrontal gyrus, paracentral gyrus, posterior cingulate cortex, and transverse temporal gyrus in the left hemisphere. These regions are highlighted in Fig. 10.

An unusual feature of the values in Table 1 is that two values are not within the range of 2.0–3.0. Most definitions of fractal dimension imply that the value must be lower than the embedding dimension, which is 3.0 for a 3-dimensional surface (Mehaute, 1991). However,

the definition of fractal dimension used here is not the exact Hausdorff dimension, thus can result in values outside this range. In the right hemisphere, the frontal pole region defies this rule. It is a highly folded gyral region that contains a relatively small number of polygons, and this deviation may be due to loss of resolution in that area.

The local FD maps revealed that the lower overall complexity in the right hemisphere was attributable to differences in the parietal and temporal lobes (Fig. 11). Local complexity was also lower for the prefrontal and temporal cortex in the left hemisphere, but only prefrontal ROIs in the left hemisphere showed significantly lower FD in the patient group.

##### Discussion

*Surface complexity in schizophrenia.* For the whole hemisphere, complexity analysis of the schizophrenia patient group revealed a global reduction in surface complexity in the right hemisphere only. This lateralization corresponds with some previous studies that detected lateralized gray matter reductions in the right hemisphere (Pantelis et al., 2003). Even so, some studies detected gray matter deficits only in the left hemisphere (Honea et al., 2005; Hulshoff Pol et al., 2006). Furthermore, prior studies of cortical folding found either bilateral or left-hemisphere reductions in GI for the schizophrenia patient group (Sallet et al., 2003) or no differences (Noga et al., 1995). Measuring the FD of a skeleton representing the cortical folding pattern revealed significantly lower FD values for both hemispheres in

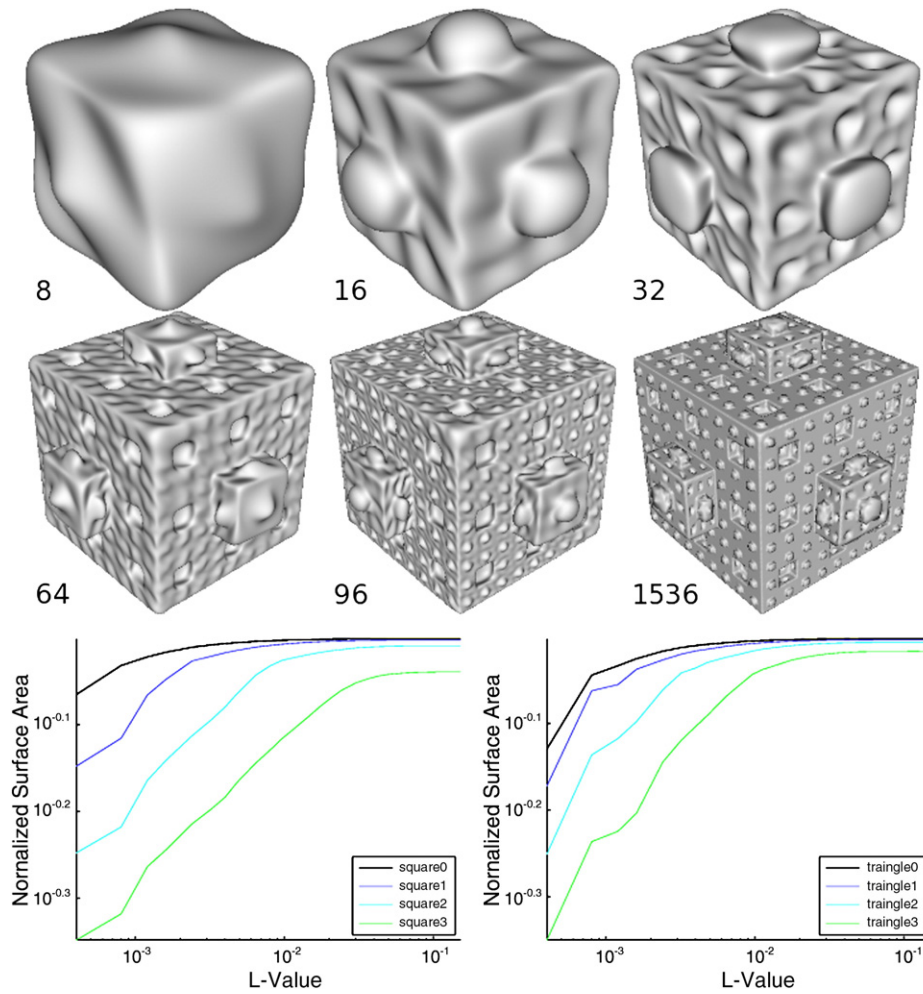


**Fig. 5.** Fractal dimension may be computed from a series of SPH low-pass filtered reconstructed surfaces. Top two rows: we show a series of level-3 cubic surfaces with projection scale of 2.0 that have been low-pass filtered; the numbers indicate the maximum  $l$ -value used in the filter. Below, we plot the normalized surface area versus the maximum  $l$ -value on a log–log scale, for detail levels 0–3. Fractal dimension can be estimated by measuring the slope over a range of  $l$ -values that results in an approximately linear function. The surface area of the reconstructed surface is divided by the surface area of the original mesh.

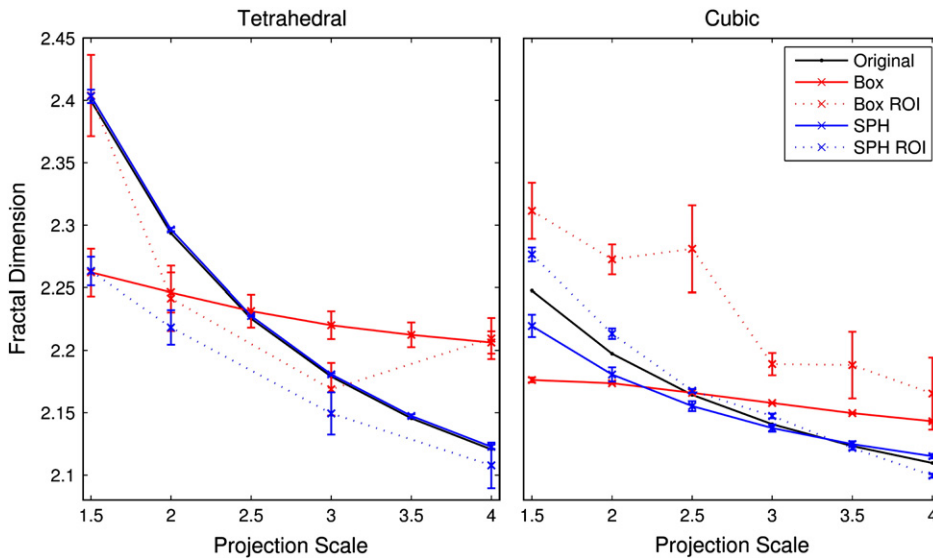


**Fig. 6.** Global and regional fractal dimension measurements obtained from spherical harmonic reconstructions are more accurate than those obtained from the box-counting approach. The average FD values – shown with standard errors of the means (SEM) – are averaged from three levels of complexity for each projection scale. Regional (ROI) values are obtained from averaged local FD values from a combined surface in which each face uses a different projection scale.

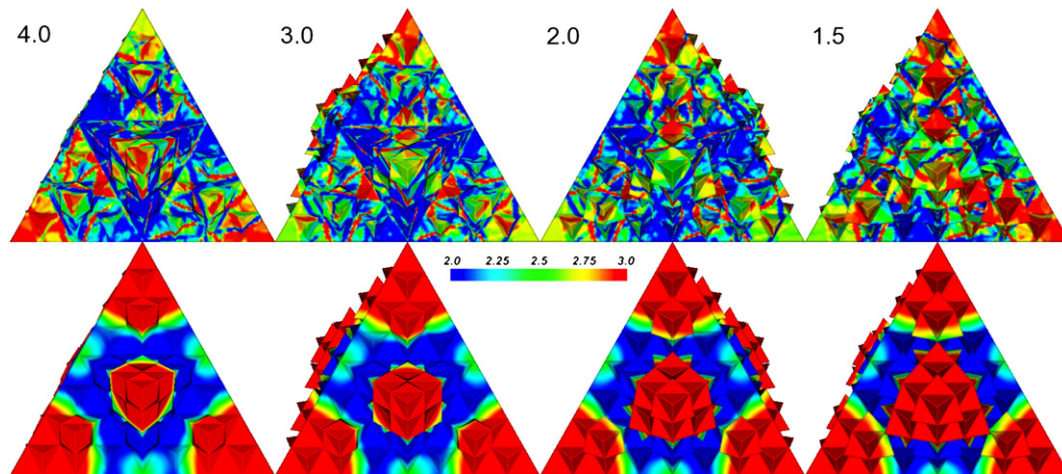


**Fig. 7.** A map of local fractal dimension based on the box-counting (top row) and spherical harmonics (bottom row) methods was calculated for a von Koch surface with varying projection scales on each surface. The level-3 surface is shown here, and the numbers represent the projection scale of each face, such that face 1.5 has the largest features. The spherical harmonic mapping clearly marks structures with higher complexity with a larger fractal dimension value, while the box-counting approach depends strongly upon the re-sampled points.

the patient group (Ha et al., 2005). This was similar to the result found using box-counting estimation of FD for the boundary between GM and WM (Bullmore et al., 1994). However, another study found an increase in FD for both hemispheres (Sandu et al., 2008). Since these complexity measures were of the GM/WM boundary, however, they may not account for any possible gray matter abnormalities and may have a different etiology.

The pattern of regional structural differences in schizophrenia versus controls is even more heterogeneous across studies, both in terms of gray matter reduction (Weinberger and McClure, 2002) and in gyrification index (Wheeler and Harper, 2007). However, the most consistently reported findings include gray matter reduction in the temporal (Goldman et al., 2008; Honea et al., 2005; McDonald et al., 2006; Wright et al., 2000) and frontal lobes (Honea et al., 2008; Thompson et al., 2009), along with an increase in the size of the lateral ventricles (Steen et al., 2006). Regional complexity analysis revealed significant decreases in complexity for the frontal lobe areas in both hemispheres, which is similar to previous studies reporting bilateral complexity differences in the frontal cortex (Narr et al., 2001); however, another study showed only right hemisphere GI increases in the prefrontal cortex (Vogeley et al., 2000; Vogeley et al., 2001).

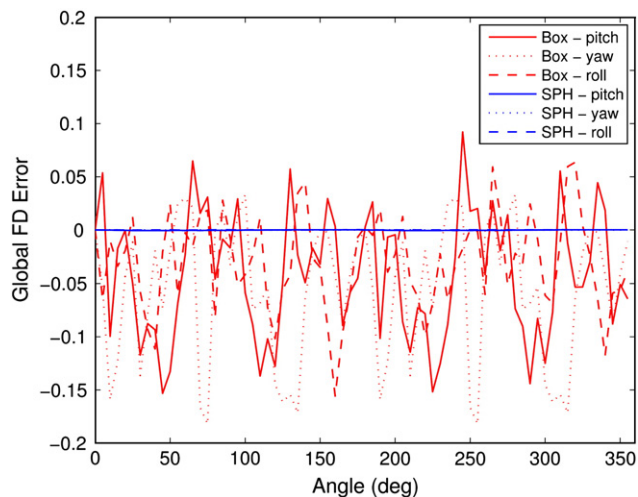


**Fig. 8.** The global fractal dimension value can depend upon the orientation of a brain surface. Rotating one brain surface around the three axes results in relatively large errors in global fractal dimension values for the box-counting approach, while the errors remain vanishingly small for the proposed spherical harmonic approach.

The evaluation of the clinical results is further complicated by the fact that the underlying pathogenetic causes for schizophrenia are heterogeneous. For example, disturbances in neurodevelopment might be influenced by genetic factors or obstetric complications, which might lead to different patterns of FD change compared to those patients who have little genetic risk but suffer a “second hit,” e.g., during adolescence. It is therefore necessary to conceive of multiple subsyndromes within schizophrenia. Hence, when all patients are analyzed as a single group, any structural abnormalities potentially related to specific subsyndromes are lost or greatly diluted. Furthermore, our local FD analyses were not corrected for multiple comparisons, and were provided solely to demonstrate that this methodological approach can calculate highly localized complexity values. To further complicate the analysis, direct comparison to GI or gray matter volume reduction cannot be made, since the complexity is a different type of measure (Thompson et al., 2005). This last point is discussed below in more detail.

Dividing patients according to the subtypes defined in DBM-IIIIR or DSM-IV diagnostic criteria may be limited by the fact that the cross-sectional psychopathology could vary from one psychotic episode to another, hence obscuring the identification of the causal pathogenetic mechanism (Gaser et al., 2004). However, using voxel-based morphometry, we have previously demonstrated that there is considerable brain structural variation related to symptom profiles, especially for the prefrontal cortex, thalamus, and temporal lobe (Nenadic et al., 2010).

The heterogeneity of these findings suggest that there is further improvements to be made in both defining schizophrenia as a psychiatric disease and in developing a standardized method to measure potentially small structural differences. It could be argued that the contradictory results are entirely due to methodological differences, diverse patient groups, or small sample sizes. It is also possible, as in any study, that unmodeled confounds mediate the differences. The algorithm proposed in this paper may overcome some of the methodological difficulties for measuring cortical surface complexity. It computes localized maps of complexity values that may be used to generate surface patterns. When combined with machine learning approaches, these patterns may be able to accurately classify certain disease states (Sun et al., 2009).

*Interpretation of surface complexity measures.* In order to clinically interpret a difference in measured complexity, it is important to be able to relate the value to a more conventionally accepted structural difference. Unlike gray matter differences, cortical thickness, or

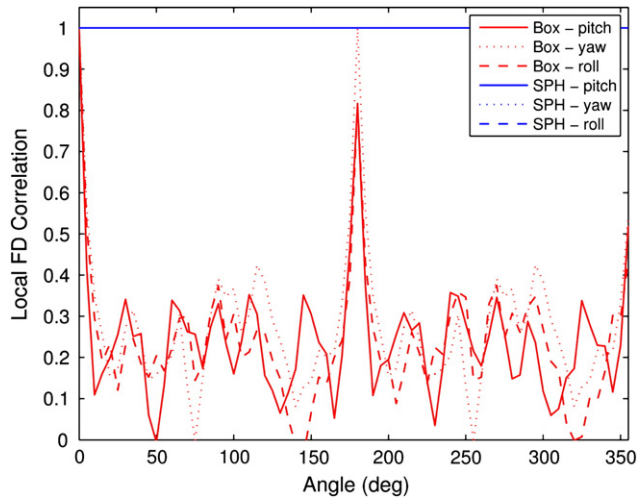


**Fig. 9.** Despite rotation along axes, the correlation between the derived local fractal dimension values and the original values from the un-rotated surface should remain (nearly) perfect. For the spherical harmonic approach, the correlation is unaffected by the rotation and is never lower than 1. However, only a rotation of 180° results in a correlation approaching a value of 1 for the box-counting approach.

cortical folding differences, surface complexity, especially at a local level, measures a structural aspect that is perhaps somewhat less intuitive or less commonly considered. It helps to bear in mind that a complexity measure does not directly measure the intuitive meaning of complexity (e.g., more detail), but is a characteristic of the surface shape. This is true at the global level, and an assumption made in the above analyses is that these concepts apply to the local level as well.

**Table 1**  
Mean annotated FD for schizophrenia and control subjects, over regions defined using registration algorithms included in the FreeSurfer software suite.

Region of interest	Left hemisphere		Right hemisphere	
	Control	Schizo.	Control	Schizo.
Bankssts	2.8153	2.7792	2.8798	2.8469
Caudal anterior cingulate	2.2952	2.2453 *	2.0625	2.0415
Caudal middle frontal	2.7336	2.7315	2.6758	2.6612
Corpus callosum	2.1758	2.1634	2.5480	2.5117 *
Cuneus	2.6512	2.6982 *	2.7209	2.7543
Entorhinal	2.9031	2.9213	2.3385	2.3477
Fusiform	2.5298	2.5095	2.4728	2.4654
Inferior parietal	2.6915	2.7035	2.6445	2.6269
Inferior temporal	2.4693	2.4659	2.5267	2.5152
Isthmus cingulate	2.1848	2.2214 *	2.7489	2.7448
Lateral occipital	2.5052	2.5074	2.4796	2.4827
Lateral orbitofrontal	2.2668	2.2838 *	2.3558	2.3514
Lingual	2.5998	2.5825	2.6844	2.6466 *
Medial orbitofrontal	2.4208	2.4476	2.3982	2.3925
Middle temporal	2.6783	2.6869	2.8799	2.8892
Parahippocampal	2.9080	2.9134	2.5354	2.5018
Paracentral	2.4777	2.5018 *	2.9015	2.9011
Parsopercularis	2.7605	2.7487	2.1845	2.1965
Parsorbitalis	2.9648	2.9595	2.2902	2.2839
Parstriangularis	2.7767	2.7454	2.5394	2.5402
Pericalcarine	2.5802	2.5523	2.8569	2.8436
Postcentral	2.7710	2.7535	2.4979	2.5104
Posterior cingulate	2.4359	2.4832 *	2.4682	2.4562
Precentral	2.7302	2.7100 *	2.5844	2.5687 *
Precuneus	2.5641	2.5463	2.7135	2.6881
Rostral anterior cingulate	2.1129	2.0976	2.3120	2.3151
Rostral middle frontal	2.5854	2.5943	2.5850	2.5776
Superior frontal	2.3807	2.3631 *	2.7530	2.7441
Superior parietal	2.6669	2.6560	2.7326	2.6679 **
Superior temporal	2.7873	2.7694	2.4479	2.4389
Supramarginal	2.6262	2.6221	2.4442	2.4397
Frontal pole	2.7954	2.7510 *	3.1806	3.2177
Temporal pole	2.8107	2.8225	2.5500	2.5780
Transverse temporal	2.6422	2.7777 *	1.9581	1.9695

\*  $p < 0.05$ , uncorrected.  
\*\*  $p < 0.05$ , FDR.

Indeed, quantitative support for this assumption is provided by the relative accuracy of regional fractal dimension differences for the combined von Koch surfaces.

A fractal is a structure that is self-similar across a range of scales, and the complexity analysis roughly corresponds to how “space-filling” the fractal surface is. However, a plot of local complexity measures for two brains – one with a large FD and one with a small FD – demonstrates that the relationship between self-similarity, space-filling, and cortical folding pattern is not particularly straightforward at the local level (Fig. 12). Generally, regions with a high FD value appear to be more periodically spaced, such as a sine wave with regular peaks and troughs. This may be because the more periodically spaced structures also tend to fill more space over the range of scales examined for derivation of complexity values. As support for this concept, the Pearson correlation coefficient between the summed fractal dimension for both hemispheres and the ratio of surface area to volume for the entire brain is significantly positive ( $r = 0.4906$ ,  $n = 195$ ,  $p = 1.67 \times 10^{-13}$ ). Further evidence comes from examining the change in fractal dimension for each surface. In the above analysis,

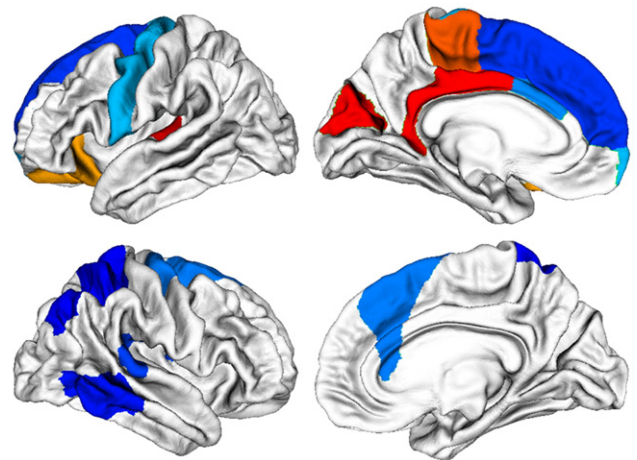


**Fig. 10.** The highlighted regions have significantly different FD values, on average, between schizophrenia and control subjects. The FD values were significantly different in the precentral gyrus, caudal anterior cingulate gyrus, frontal pole, cuneus, isthmus cingulate gyrus, lateral orbitofrontal gyrus, paracentral gyrus, posterior cingulate cortex, and transverse temporal gyrus in the left hemisphere; and the precentral gyrus, corpus callosum, lingual gyrus, and superior parietal lobe in the right hemisphere. Blue colors indicate that the mean values for the schizophrenia group are lower than those for the control group.

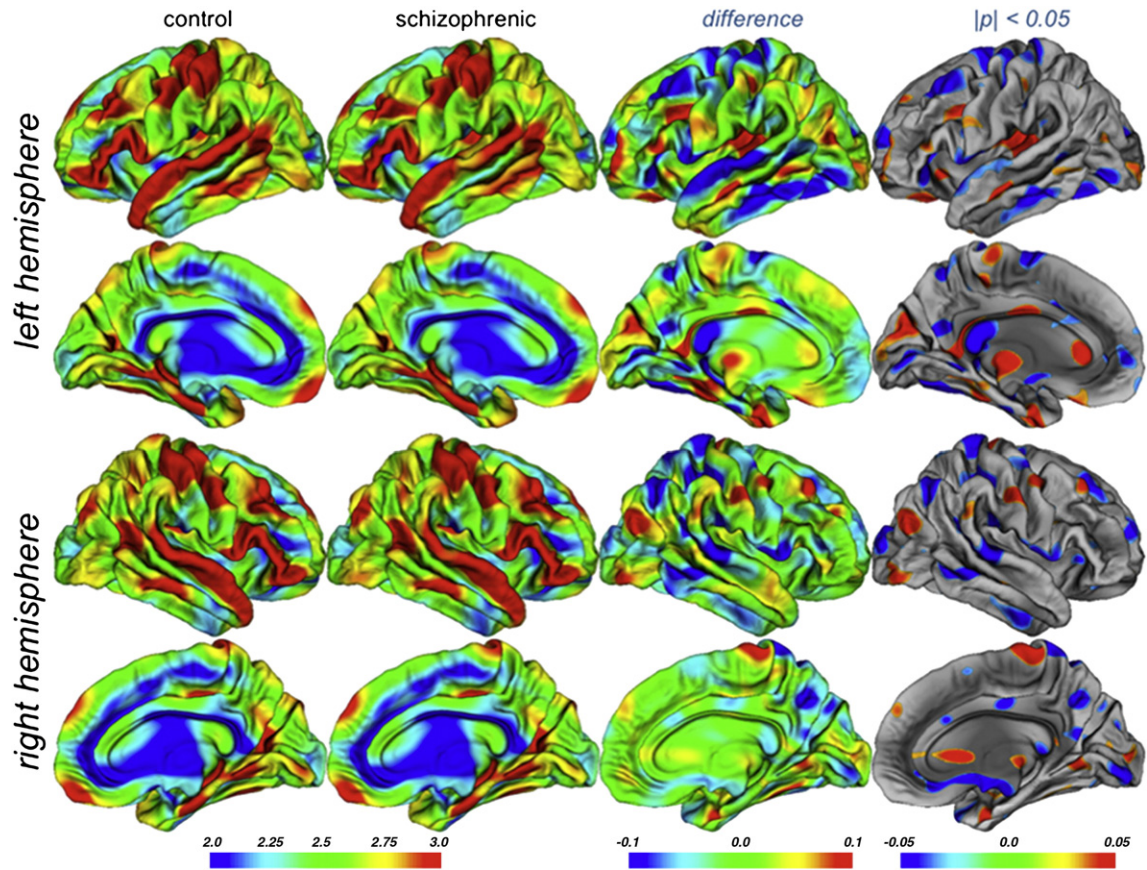


**Fig. 11.** Local average FD values are mapped onto a representative cortical surface model for control and schizophrenia groups. Left and right hemispheres are shown. A map of mean complexity differences (3rd column) between groups and  $p$ -values showing the local significance of the inter-group difference are shown (4th column). Vertices are highlighted if (uncorrected)  $p < 0.05$ . For both the mean group difference and  $p$ -value maps, blue colors indicate that the mean values for the schizophrenia group are lower than those for the control group.

the central surface was used rather than the white matter or pial surfaces. The fractal dimensions of these surfaces were relatively stably offset from the fractal dimension value of the central surface, such that the pial surfaces had higher fractal dimension values and the white matter surfaces had lower values (Fig. S2). Again, this may be due to the more (or less) space-filling structure of the pial (or white) surfaces as compared with the central surface.

The measured FD value for an object depends, to some extent, on the range of scales examined, and may depend upon the resolution of the re-sampling, or the largest  $l$ -value in the case of spherical

harmonic reconstructions. A very high resolution re-sampling could retain high-frequency noise that may be due more to noise in the scan or the reconstruction protocol than biological aspects of brain structure. For this reason, we deliberately used fairly low-frequency reconstructions such that the underlying base shape determines the resulting FD value. This avoidance of very high frequency information should make our approach less dependent on scanner or noise. When this was tested, the FD value was not completely independent of scanner, as intensity differences are reflected to some extent in structural differences in the reconstructed surface mesh. Scanner

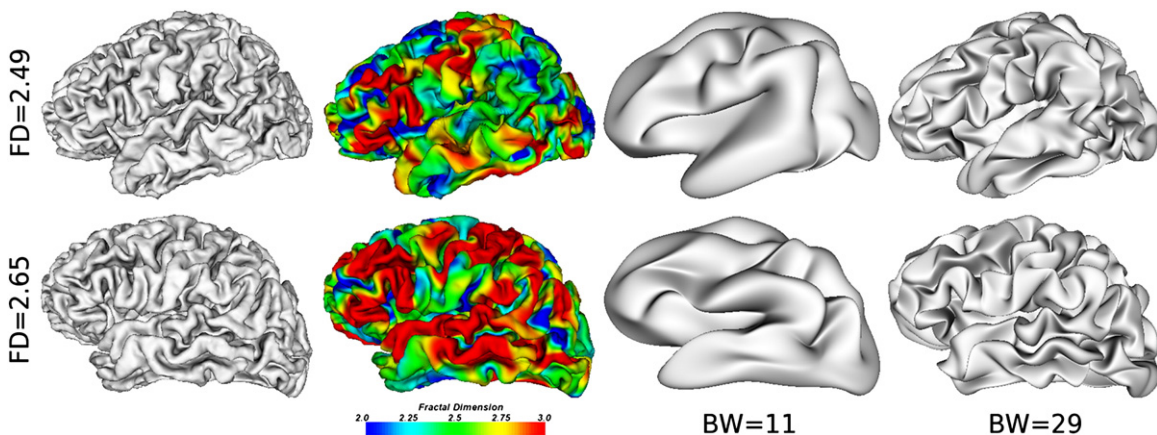


**Fig. 12.** These two example surfaces have very different cortical complexity values. To visualize what a complexity value means in terms of structure, two low-pass filtered reconstructions are shown, as well as a local complexity map. In regions of high complexity, the underlying brain structure is more regular, similar to a sine wave, which is most apparent in the temporal and frontal lobes.

biases may influence pre-processing steps such as segmentation and surface reconstruction. If that is the case, these biases are then inevitably reflected in the resulting FD value, but should not induce systematic differences between groups of patients and controls. However, the pattern of local FD values for the same brain scanned with different scanners appears to be highly reproducible (Fig. S3).

**Conclusion**

In this paper, we proposed a new approach to measure cortical surface complexity from brain surface meshes. The approach relies on highly smoothed spherical harmonic reconstructions to derive complexity values, using a new definition of fractal dimension as the regression of  $\log(\text{surface area})$  versus  $\log(\text{max } l\text{-value})$ . Despite the new definition, the fractal dimension values can accurately measure differences in global (or overall) fractal dimension, and is demonstrably more accurate than the box-counting method. The new definition is also consistent for this method, thus allowing potential comparison of results from multiple studies.

Because the number of vertices in each construction remains the same, calculation of local (vertex-wise) complexity values is straightforward. These local values can be used to obtain regional complexity values by averaging the values from vertices contained within each region of interest. Using artificial von Koch surfaces, we demonstrated that the regional values followed the trend for differences in fractal dimension (i.e., a plot of projection scale versus fractal dimension remained monotonic). Visual inspection of local FD maps on the von Koch surfaces revealed a highly regular pattern.

As demonstrated in the rotated cortical surface, the box-counting method must be preceded by careful feature alignment of the cortical surfaces to attempt to map re-parameterized points to equivalent locations across subjects (Thompson et al., 1996). Due to the high-resolution re-sampling in the spherical harmonic approach, we could bypass this step without loss of accuracy in global and local complexity measures. However, to minimize variability, subjects were registered to a common template before analysis.

Cortical surface complexity may be a valid clinical marker for schizophrenia (Narr et al., 2004), Williams syndrome (Gaser et al., 2006; Thompson et al., 2005), bipolar disorder (McIntosh et al., 2009), and obsessive-compulsive disorder (Ha et al., 2005). When applied to a large sample of schizophrenia and control subjects, the schizophrenia subjects had significantly lower cortical surface complexity in the right hemisphere. Regional and local analyses suggest that there are differences in the frontal, parietal, and temporal lobes, which should be examined in more detail. These preliminary findings demonstrate that our approach can detect relatively small, local differences in complexity.

Supplementary materials related to this article can be found online at doi:10.1016/j.neuroimage.2011.02.007.

**Acknowledgments**

R. A. Y., G. Z., and C. G. were supported by grants BMBF 01EV0709 and BMBF 01GW0740 from the German Bundesministerium für Bildung und Forschung. P.T. was supported by NIH grants EB008432, EB008281, EB007813, HD050735. I.N. was partly supported through the EU grant: RTN, FP6; "EUTwinS," MRTN-CT-2006-035987.

**Appendix. Spherical harmonic analysis**

To analyze the harmonic content of a surface mesh, the first required step is to change the parameter space from Cartesian to spherical coordinates  $\theta$  and  $\phi$ , where  $\theta$  is the co-latitude and  $\phi$  is the azimuthal coordinate. The original spherical mapping is from the standard FreeSurfer pipeline. Then, grid points are interpolated for equally sampled values of  $\theta$  and  $\phi$  for all members in the sets, such that there are  $2B$  points per set, where  $B$  is the degree, or maximum  $l$ -

value. For each regularly sampled point, the closest polygon on the spherical mapping is found. Within the closest polygon, a spatial location for the interpolated vertex is approximated using barycentric coordinates. The result is a regularly sampled spherical map in which every point is associated with a coordinate that gives its location on the original surface.

Once the surface mesh is re-parameterized, the harmonic content of a spherical mesh may be obtained using normalized spherical harmonics  $Y_l^m(\theta, \phi)$ :

$$Y_l^m(\theta, \phi) = P_l^m(\cos \theta)e^{im\phi}, \tag{3}$$

where  $l$  and  $m$  are integers with  $|m| \leq l$ , and  $P_l^m$  is the associated Legendre function defined by:

$$P_l^m(x) = \frac{1}{2^l l!} (1-x^2)^{\frac{m}{2}} \frac{d^{l+m}}{dx^{l+m}} (x^2-1)^l. \tag{4}$$

A square-integrable function  $f(\theta, \phi)$  on the sphere may be expanded in the spherical harmonic basis such that:

$$f(\theta, \phi) = \sum_{l=0}^B \sum_{m=-l}^l \|Y_l^m\|_2^{-2} \hat{f}(l, m) \cdot Y_l^m, \tag{5}$$

where the coefficients  $\hat{f}(l, m)$  are defined by  $\hat{f}(l, m) = \langle f, Y_l^m \rangle$  and the  $L^2$ -norm of  $Y_l^m$  is given by:

$$\|Y_l^m\|_2^{-2} = \frac{4\pi}{2l+1} \cdot \frac{(l+m)!}{(l-m)!}. \tag{6}$$

It is possible to solve this system directly by finding the coefficients first, but a more efficient approach is to use a divide-and-conquer scheme (Healy et al., 1996).

These coefficients can then be low-pass filtered, such that only lower frequencies have non-zero values, and passed through an inverse transform to produce a surface reconstruction. For FD calculations, ten reconstructions are produced using an upper  $l$ -value between 11 and 29.

**References**

Andreasen, N.C., Arndt, S., Alliger, R., Miller, D., Flaum, M., 1995. Symptoms of schizophrenia: methods, meanings, and mechanisms. *Arch. Gen. Psychiatry* 52, 341–351.

Awate, S., Win, L., Yushkevich, P., Schultz, R., Gee, J., 2008. 3D cerebral cortical morphometry in autism: increased folding in children and adolescents in frontal, parietal, and temporal lobes. In: Metaxas, D., Axel, L., Fichtinger, G., Székely, G. (Eds.), *Medical Image Computing and Computer-Assisted Intervention – MICCAI 2008*. Springer Berlin, Heidelberg, pp. 559–567.

Awate, S., Yushkevich, P., Licht, D., Gee, J., 2009. Gender differences in cerebral cortical folding: multivariate complexity-shape analysis with insights into handling brain-volume differences. In: Yang, G.-Z., Hawkes, D., Rueckert, D., Noble, A., Taylor, C. (Eds.), *Medical Image Computing and Computer-Assisted Intervention – MICCAI 2009*. Springer Berlin, Heidelberg, pp. 200–207.

Awate, S.P., Yushkevich, P.A., Song, Z., Licht, D.J., Gee, J.C., 2010. Cerebral cortical folding analysis with multivariate modeling and testing: studies on gender differences and neonatal development. *Neuroimage* 53, 450–459.

Benjamini, Y., Hochberg, Y., 1995. Controlling the false discovery rate: a practical and powerful approach to multiple testing. *J. R. Stat. Soc. B Methodol.* 57, 289–300.

Blanton, R.E., Levitt, J.G., Thompson, P.M., Narr, K.L., Capetillo-Cunliffe, L., Nobel, A., Singerman, J.D., McCracken, J.T., Toga, A.W., 2001. Mapping cortical asymmetry and complexity patterns in normal children. *Psychiatry Res. Neuroimaging* 107, 29–43.

Bullmore, E., Brammer, M., Harvey, I., Persaud, R., Murray, R., Ron, M., 1994. Fractal analysis of the boundary between white matter and cerebral cortex in magnetic resonance images: a controlled study of schizophrenic and manic-depressive patients. *Psychol. Med.* 24, 771–781.

Casanova, M.F., Daniel, D.G., Goldberg, T.E., Suddath, R.L., Weinberger, D.R., 1989. Shape analysis of the middle cranial fossa of schizophrenic patients: a computerized tomographic study. *Schizophr. Res.* 2, 333–338.

Chung, M.K., Robbins, S.M., Dalton, K.M., Davidson, R.J., Alexander, A.L., Evans, A.C., 2005. Cortical thickness analysis in autism with heat kernel smoothing. *Neuroimage* 25, 1256–1265.

Dale, A.M., Fischl, B., Sereno, M.I., 1999. Cortical surface-based analysis: I. Segmentation and surface reconstruction. *NeuroImage* 9, 179–194.

- Davatzikos, C., Shen, D., Gur, R.C., Wu, X., Liu, D., Fan, Y., Hughett, P., Turetsky, B.I., Gur, R. E., 2005. Whole-brain morphometric study of schizophrenia revealing a spatially complex set of focal abnormalities. *Arch. Gen. Psychiatry* 62, 1218–1227.
- Esteban, F.J., Sepulcre, J., de Mendizbal, N.V., Goñi, J., Navas, J., Miras, J.R., Bejarano, B., Masdeu, J.C., Villoslada, P., 2007. Fractal dimension and white matter changes in multiple sclerosis. *Neuroimage* 36, 543–549.
- Esteban, F.J., Sepulcre, J., Ruiz de Miras, J., Navas, J., Velez de Mendizabal, N., Goni, J., Bejarano, B., Villoslada, P., 2009. Fractal dimension analysis of grey matter in multiple sclerosis. *J. Neurol. Sci.* 282, 67–71.
- Fischl, B., Dale, A.M., 2000. Measuring the thickness of the human cerebral cortex from magnetic resonance images. *Proc. Natl Acad. Sci. USA* 97, 11050–11055.
- Fischl, B., Sereno, M.I., Dale, A.M., 1999a. Cortical surface-based analysis: II. Inflation, flattening, and a surface-based coordinate system. *Neuroimage* 9, 195–207.
- Fischl, B., Sereno, M.I., Tootell, R.B.H., Dale, A.M., 1999b. High-resolution intersubject averaging and a coordinate system for the cortical surface. *HBM* 8, 272–284.
- Free, S.L., Sisodiya, S.M., Cook, M.J., Fish, D.R., Shorvon, S.D., 1996. Three-dimensional fractal analysis of the white matter surface from magnetic resonance images of the human brain. *Cereb. Cortex* 6, 830–836.
- Gaser, C., Luders, E., Thompson, P.M., Lee, A.D., Dutton, R.A., Geaga, J.A., Hayashi, K.M., Bellugi, U., Galaburda, A.M., Korenberg, J.R., Mills, D.L., Toga, A.W., Reiss, A.L., 2006. Increased local gyrification mapped in Williams syndrome. *Neuroimage* 33, 46–54.
- Gaser, C., Nenadic, I., Volz, H.-P., Buchel, C., Sauer, H., 2004. Neuroanatomy of 'hearing voices': a frontotemporal brain structural abnormality associated with auditory hallucinations in schizophrenia. *Cereb. Cortex* 14, 91–96.
- Goldman, A.L., Pezawas, L., Mattay, V.S., Fischl, B., Verchinski, B.A., Zolnick, B., Weinberger, D.R., Meyer-Lindenberg, A., 2008. Heritability of brain morphology related to schizophrenia: a large-scale automated magnetic resonance imaging segmentation study. *Biol. Psychiatry* 63, 475–483.
- Gutman, B., Wang, Y., Morra, J., Toga, A.W., Thompson, P.M., 2009. Disease classification with hippocampal shape invariants. *Hippocampus* 19, 572–578.
- Ha, T.H., Yoon, U., Lee, K.J., Shin, Y.W., Lee, J.-M., Kim, I.Y., Ha, K.S., Kim, S.I., Kwon, J.S., 2005. Fractal dimension of cerebral cortical surface in schizophrenia and obsessive-compulsive disorder. *Neurosci. Lett.* 384, 172–176.
- Healy, D.M., Rockmore, D.N., Moore, S.S.B., 1996. FFTs for the 2-Sphere-Improvements and Variations. Dartmouth College.
- Honea, R., Crow, T.J., Passingham, D., Mackay, C.E., 2005. Regional deficits in brain volume in schizophrenia: a meta-analysis of voxel-based morphometry studies. *Am. J. Psychiatry* 162, 2233–2245.
- Honea, R.A., Meyer-Lindenberg, A., Hobbs, K.B., Pezawas, L., Mattay, V.S., Egan, M.F., Verchinski, B., Passingham, R.E., Weinberger, D.R., Callicott, J.H., 2008. Is gray matter volume an intermediate phenotype for schizophrenia? A voxel-based morphometry study of patients with schizophrenia and their healthy siblings. *Biol. Psychiatry* 63, 465–474.
- Hulshoff Pol, H.E., Schnack, H.G., Mandl, R.C.W., Brans, R.G.H., van Haren, N.E.M., Baaré, W.F.C., van Oel, C.J., Collins, D.L., Evans, A.C., Kahn, R.S., 2006. Gray and white matter density changes in monozygotic and same-sex dizygotic twins discordant for schizophrenia using voxel-based morphometry. *Neuroimage* 31, 482–488.
- Im, K., Lee, J.-M., Yoon, U., Shin, Y.-W., Hong, S.B., Kim, I.Y., Kwon, J.S., Kim, S.I., 2006. Fractal dimension in human cortical surface: multiple regression analysis with cortical thickness, sulcal depth, and folding area. *Hum. Brain Mapp.* 27, 994–1003.
- Jiang, J., Zhu, W., Shi, F., Zhang, Y., Lin, L., Jiang, T., 2008. A robust and accurate algorithm for estimating the complexity of the cortical surface. *J. Neurosci. Meth.* 172, 122–130.
- Kalmanti, E., Maris, T.G., 2007. Fractal dimension as an index of brain cortical changes throughout life. *In Vivo* 21, 641–646.
- Kawasaki, Y., Suzuki, M., Kherif, F., Takahashi, T., Zhou, S.-Y., Nakamura, K., Matsui, M., Sumiyoshi, T., Seto, H., Kurachi, M., 2007. Multivariate voxel-based morphometry successfully differentiates schizophrenia patients from healthy controls. *Neuroimage* 34, 235–242.
- King, R., George, A., Jeon, T., Hynan, L., Youn, T., Kennedy, D., Dickerson, B., 2009. Characterization of atrophic changes in the cerebral cortex using fractal dimensional analysis. *Brain Imaging Behav.* 3, 154–166.
- King, R.D., Brown, B., Hwang, M., Jeon, T., George, A.T., 2010. Fractal dimension analysis of the cortical ribbon in mild Alzheimer's disease. *Neuroimage* 53, 471–479.
- Kiselev, V.G., Hahn, K.R., Auer, D.P., 2003. Is the brain cortex a fractal? *Neuroimage* 20, 1765–1774.
- Kostelec, P.J., Maslen, D.K., Dennis, M., Healy, J., Rockmore, D.N., 2000. Computational harmonic analysis for tensor fields on the two-sphere. *J. Comput. Phys.* 162, 514–535.
- Lee, J.-M., Yoon, U., Kim, J.-J., Kim, I.Y., Lee, D.S., Kwon, J.S., Kim, S.I., 2004. Analysis of the hemispheric asymmetry using fractal dimension of a skeletonized cerebral surface. *IEEE Trans. Biomed. Eng.* 51, 1494–1498.
- Liu, J.Z., Zhang, L.D., Yue, G.H., 2003. Fractal dimension in human cerebellum measured by magnetic resonance imaging. *Biophys. J.* 85, 4041–4046.
- Lopes, R., Bétrouni, N., 2009. Fractal and multifractal analysis: a review. *Med. Image Anal.* 13, 634–649.
- Luders, E., Narr, K.L., Thompson, P.M., Rex, D.E., Jancke, L., Steinmetz, H., Toga, A.W., 2004. Gender differences in cortical complexity. *Nat. Neurosci.* 7, 799–800.
- Luders, E., Thompson, P.M., Narr, K.L., Toga, A.W., Jancke, L., Gaser, C., 2006. A curvature-based approach to estimate local gyrification on the cortical surface. *Neuroimage* 29, 1224–1230.
- Lui, L.M., Wong, T.W., Zeng, W., Gu, X., Thompson, P.M., Chan, T.F., Yau, S.T., 2010. Detection of shape deformities using Yamabe flow and Beltrami coefficients. *Inverse Probl. Imaging* 4, 311–333.
- MacDonald, D., Kabani, N., Avis, D., Evans, A.C., 2000. Automated 3-D extraction of inner and outer surfaces of cerebral cortex from MRI. *Neuroimage* 12, 340–356.
- Mandelbrot, B.B., Blumen, A., 1989. Fractal geometry: what is it, and what does it do? [and Discussion]. *Proceedings of the Royal Society of London. Series A. Math. Phys. Sci.* 423, 3–16.
- Mangin, J.-F., Frouin, V., Bloch, I., Régis, J., López-Krahe, J., 1995. From 3D magnetic resonance images to structural representations of the cortex topography using topology preserving deformations. *J. Math. Imaging Vis.* 5, 297–318.
- McDonald, C., Marshall, N., Sham, P.C., Bullmore, E.T., Schulze, K., Chapple, B., Bramon, E., Filbey, F., Quraishi, S., Walshe, M., Murray, R.M., 2006. Regional brain morphometry in patients with schizophrenia or bipolar disorder and their unaffected relatives. *Am. J. Psychiatry* 163, 478–487.
- McIntosh, A.M., Moorhead, T.W.J., McKirdy, J., Hall, J., Sussmann, J.E.D., Stanfield, A.C., Harris, J.M., Johnstone, E.C., Lawrie, S.M., 2009. Prefrontal gyral folding and its cognitive correlates in bipolar disorder and schizophrenia. *Acta Psychiatr. Scand.* 119, 192–198.
- Mehaute, A.L., 1991. Fractal geometries: theory and applications. CRC Press, Boca Raton, FL.
- Morra, J.H., Tu, Z., Apostolova, L.G., Green, A.E., Avedissian, C., Madsen, S.K., Parikshak, N., Hua, X., Toga, A.W., Jack, C.R., Schuff, N., Weiner, M.W., Thompson, P.M., 2009. Automated 3D mapping of hippocampal atrophy and its clinical correlates in 400 subjects with Alzheimer's disease, mild cognitive impairment, and elderly controls. *Hum. Brain Mapp.* 30, 2766–2788.
- Narr, K.L., Bilder, R.M., Kim, S., Thompson, P.M., Szaszko, P., Robinson, D., Luders, E., Toga, A.W., 2004. Abnormal gyral complexity in first-episode schizophrenia. *Biol. Psychiatry* 55, 859–867.
- Narr, K.L., Thompson, P.M., Sharma, T., Moussai, J., Zoumalan, C., Rayman, J., Toga, A.W., 2001. Three-dimensional mapping of gyral shape and cortical surface asymmetries in schizophrenia: gender effects. *Am. J. Psychiatry* 158, 244–255.
- Nenadic, I., Sauer, H., Gaser, C., 2010. Distinct pattern of brain structural deficits in subsyndromes of schizophrenia delineated by psychopathology. *Neuroimage* 49, 1153–1160.
- Noga, J.T., Aylward, E., Barta, P.E., Pearlson, G.D., 1995. Cingulate gyrus in schizophrenic patients and normal volunteers. *Psychiatry Res. Neuroimaging* 61, 201–208.
- Oldfield, R.C., 1971. The assessment and analysis of handedness: the Edinburgh inventory. *Neuropsychologia* 9, 97–113.
- Pantelis, C., Velakoulis, D., McGorry, P., Wood, S., Suckling, J., Phillips, L., Yung, A., Bullmore, E., Brewer, W., Soulsby, B., Desmond, P., McGuire, P., 2003. Neuroanatomical abnormalities before and after onset of psychosis: a cross-sectional and longitudinal MRI comparison. *Lancet* 361, 281–288.
- Sallet, P.C., Elks, H., Alves, T.M., Oliveira, J.R., Sassi, E., de Castro, C.C., Busatto, G.F., Gattaz, W.F., 2003. Reduced cortical folding in schizophrenia: an MRI morphometric study. *Am. J. Psychiatry* 160, 1606–1613.
- Sandu, A.-L., Rasmussen, Lundervold, A., Kreuder, F., Neckelmann, G., Hugdahl, K., Specht, K., 2008. Fractal dimension analysis of MR images reveals grey matter structure irregularities in schizophrenia. *Comput. Med. Imaging Graph.* 32, 150–158.
- Schaer, M., Cuadra, M.B., Tamarit, L., Lazeyras, F., Eliez, S., Thiran, J.P., 2008. A surface-based approach to quantify local cortical gyrification. *IEEE Trans. Med. Imaging* 27, 161–170.
- Shyu, K.K., Wu, Y.T., Chen, T.R., Chen, H.Y., Hu, H.H., Guo, W.Y., 2010. Measuring complexity of fetal cortical surface from MR images using 3-D modified box-counting method. *IEEE Trans. Instrum. Meas.* 1–10.
- Soriano-Mas, C., Pujol, J.S., Alonso, P., Cardoner, N., Menchón, J.M., Harrison, B.J., Deus, J., Vallejo, J., Gaser, C., 2007. Identifying patients with obsessive-compulsive disorder using whole-brain anatomy. *Neuroimage* 35, 1028–1037.
- Steen, R.G., Mull, C., McClure, R., Hamer, R.M., Lieberman, J.A., 2006. Brain volume in first-episode schizophrenia: systematic review and meta-analysis of magnetic resonance imaging studies. *Br. J. Psychiatry* 188, 510–518.
- Sun, D., van Erp, T.G.M., Thompson, P.M., Bearden, C.E., Daley, M., Kushan, L., Hardt, M.E., Nuechterlein, K.H., Toga, A.W., Cannon, T.D., 2009. Elucidating a magnetic resonance imaging-based neuroanatomic biomarker for psychosis: classification analysis using probabilistic brain atlas and machine learning algorithms. *Biol. Psychiatry* 66, 1055–1060.
- Thompson, P.M., Bartzokis, G., Hayashi, K.M., Klunder, A.D., Lu, P.H., Edwards, N., Hong, M.S., Yu, M., Geaga, J.A., Toga, A.W., Charles, C., Perkins, D.O., McEvoy, J., Hamer, R. M., Tohen, M., Tollefson, G.D., Lieberman, J.A., Group, T.H.S., 2009. Time-lapse mapping of cortical changes in schizophrenia with different treatments. *Cereb. Cortex* 19, 1107–1123.
- Thompson, P.M., Hayashi, K.M., Sowell, E.R., Gogtay, N., Giedd, J.N., Rapoport, J.L., de Zubicaray, G.I., Janke, A.L., Rose, S.E., Semple, J., Doddrell, D.M., Wang, Y., van Erp, T.G.M., Cannon, T.D., Toga, A.W., 2004. Mapping cortical change in Alzheimer's disease, brain development, and schizophrenia. *Neuroimage* 23, S2–S18.
- Thompson, P.M., Lee, A.D., Dutton, R.A., Geaga, J.A., Hayashi, K.M., Eckert, M.A., Bellugi, U., Galaburda, A.M., Korenberg, J.R., Mills, D.L., Toga, A.W., Reiss, A.L., 2005. Abnormal cortical complexity and thickness profiles mapped in Williams syndrome. *J. Neurosci.* 25, 4146–4158.
- Thompson, P.M., Schwartz, C., Lin, R.T., Khan, A.A., Toga, A.W., 1996. Three-dimensional statistical analysis of sulcal variability in the human brain. *J. Neurosci.* 16, 4261–4274.
- Toro, R., Perron, M., Pike, B., Richer, L., Veillette, S., Pausova, Z., Paus, T., 2008. Brain size and folding of the human cerebral cortex. *Cereb. Cortex* 18, 2352–2357.
- Vogele, K., Schneider-Axmann, T., Pfeiffer, U., Tepest, R., Bayer, T.A., Bogerts, B., Honer, W.G., Falkai, P., 2000. Disturbed gyrification of the prefrontal region in male schizophrenic patients: a morphometric postmortem study. *Am. J. Psychiatry* 157, 34–39.
- Vogele, K., Tepest, R., Pfeiffer, U., Schneider-Axmann, T., Maier, W., Honer, W.G., Falkai, P., 2001. Right frontal hypergyria differentiation in affected and unaffected siblings

- from families multiply affected with schizophrenia: a morphometric MRI study. *Am. J. Psychiatry* 158, 494–496.
- Wang, Y., Zhang, J., Gutman, B., Chan, T.F., Becker, J.T., Aizenstein, H.J., Lopez, O.L., Tamburo, R.J., Toga, A.W., Thompson, P.M., 2010. Multivariate tensor-based morphometry on surfaces: application to mapping ventricular abnormalities in HIV/AIDS. *Neuroimage* 49, 2141–2157.
- Weinberger, D., McClure, R., 2002. Neurotoxicity, neuroplasticity, and magnetic resonance imaging morphometry: what is happening in the schizophrenic brain? *Arch. Gen. Psychiatry* 59, 553–558.
- Wheeler, D.G., Harper, C.G., 2007. Localised reductions in gyrification in the posterior cingulate: schizophrenia and controls. *Prog. Neuro Psychopharmacol. Biol. Psychiatry* 31, 319–327.
- Wright, I.C., Rabe-Hesketh, S., Woodruff, P.W.R., David, A.S., Murray, R.M., Bullmore, E. T., 2000. Meta-analysis of regional brain volumes in schizophrenia. *Am. J. Psychiatry* 157, 16–25.
- Wu, Y.-T., Shyu, K.-K., Chen, T.-R., Guo, W.-Y., 2009. Using three-dimensional fractal dimension to analyze the complexity of fetal cortical surface from magnetic resonance images. *Nonlinear Dyn.* 58, 745–752.
- Wu, Y.-T., Shyu, K.-K., Jao, C.-W., Wang, Z.-Y., Soong, B.-W., Wu, H.-M., Wang, P.-S., 2010. Fractal dimension analysis for quantifying cerebellar morphological change of multiple system atrophy of the cerebellar type (MSA-C). *Neuroimage* 49, 539–551.
- Xu, C., Pham, D.L., Rettmann, M.E., Yu, D.N., Prince, J.L., 1999. Reconstruction of the human cerebral cortex from magnetic resonance images. *Med. Imaging IEEE Trans.* 18, 467–480.
- Yotter, R.A., Thompson, P.M., Gaser, C., 2010. Estimating local surface complexity maps using spherical harmonic reconstructions. In: Jiang, T. (Ed.), *MICCAI*. Springer Berlin, Beijing, China.
- Yushkevich, P., Dubb, A., Xie, Z., Gur, R., Gur, R., Gee, J., 2005. Regional structural characterization of the brain of schizophrenia patients. *Acad. Radiol.* 12, 1250–1261.
- Zhang, L., Butler, A.J., Sun, C.-K., Sahgal, V., Wittenberg, G.F., Yue, G.H., 2008a. Fractal dimension assessment of brain white matter structural complexity post stroke in relation to upper-extremity motor function. *Brain Res.* 1228, 229–240.
- Zhang, L., Dean, D., Liu, J.Z., Sahgal, V., Wang, X., Yue, G.H., 2007. Quantifying degeneration of white matter in normal aging using fractal dimension. *Neurobiol. Aging* 28, 1543–1555.
- Zhang, L., Liu, J.Z., Dean, D., Sahgal, V., Yue, G.H., 2006. A three-dimensional fractal analysis method for quantifying white matter structure in human brain. *J. Neurosci. Meth.* 150, 242–253.
- Zhang, Y., Jiang, J., Lin, L., Shi, F., Zhou, Y., Yu, C., Li, K., Jiang, T., 2008b. A surface-based fractal information dimension method for cortical complexity analysis. *Med. Imaging Augmented Real.* 133–141.
- Zilles, K., Armstrong, E., Schleicher, A., Kretschmann, H.-J., 1988. The human pattern of gyrification in the cerebral cortex. *Anat. Embryol.* 179, 173–179.